Algerian Journal of Research and Technology
https://doi.org/10.58681/ajrt.26100106
A.J.R.T Volume 10 (N°01) (2026) 53- 62

Numerical Investigation of the Hydrodynamic Performance of the Duisburg Test Case Propeller Using RANS-Based CFD Simulations

Z. Elkhaldi[1*], A. Hedd[1], L. Adjlout[1], O. Imine[1]

[1]*Marine Engineering Department, University of Science and Technologies, Oran, Algeria*

Corresponding author: **-** Zineb.elkhaldi@univ-usto.dz

Received. February 15, 2026. Accepted. March 21, 2026. Published July 25, 2026

DOI: https://doi.org/10.58681/ajrt.26100106

Abstract. This study presents a numerical investigation of the hydrodynamic performance of the Duisburg Test Case (DTC) propeller using a Reynolds-Averaged Navier–Stokes (RANS)-based Computational Fluid Dynamics (CFD) approach. The propeller geometry was reconstructed and discretized using a structured computational mesh, and the simulations were performed using the ANSYS CFX solver with the k−ω SST turbulence model and the Multiple Reference Frame (MRF) approach. The open-water performance was evaluated over a range of advance coefficients from J = 0.1 to 1.0, and the predicted thrust coefficient, torque coefficient, and open-water efficiency were compared with available experimental data. The numerical results reproduced the main trends of the experimental propeller characteristics, although noticeable differences were observed at several operating conditions. The mean absolute deviations were approximately 15.9% for K_T, 13.5% for $10K_Q$, and 12.7% for η_0. In addition, pressure distributions on the blade surfaces, pressure coefficient distributions at r/R=0.7, and the downstream wake structure were analyzed to characterize the propeller flow field. The results provide an assessment of the capability of the adopted RANS-based CFD approach to reproduce the principal hydrodynamic characteristics of the DTC propeller.

Keywords. Computational Fluid Dynamics (CFD), Duisburg Test Case (DTC), Marine Propeller, RANS Simulations, Hydrodynamic Performance.

INTRODUCTION

Marine propellers play a fundamental role in ship propulsion, and their hydrodynamic performance has a direct influence on propulsive efficiency, fuel consumption, and overall ship operating performance. The accurate prediction of propeller thrust, torque, and efficiency is therefore essential for the analysis and improvement of marine propulsion systems. Open-water propeller characteristics are commonly described in terms of the advance coefficient, thrust coefficient, torque coefficient, and open-water efficiency, which provide standardized measures for assessing propeller performance under uniform inflow conditions (ITTC, 2021; Carlton, 2018).

Experimental testing remains an important approach for determining propeller hydrodynamic characteristics and for providing reference data for the validation of numerical methods. However, experimental investigations can require considerable time and resources, while providing limited access to detailed information about the three-dimensional flow field around the propeller blades. With the continuous development of computational resources, Computational Fluid Dynamics (CFD) has consequently become an important tool for investigating marine propeller flows and predicting their hydrodynamic performance. Reynolds-Averaged Navier–Stokes (RANS) approaches are particularly attractive because they provide a practical compromise between computational cost and the ability to resolve the principal features of turbulent propeller flows (Kınacı et al., 2013). The application of RAN based CFD to marine propellers has been extensively investigated, including comparisons with experimental measurements.

Kınacı et al. (2013) investigated the propeller performance of the Duisburg Test Case (DTC) using a RANSE-based commercial CFD approach. Their study considered the propeller under open-water conditions and compared the predicted hydrodynamic characteristics with experimental data, showing good agreement between numerical and experimental results. Such benchmark-based investigations are particularly valuable because they provide a controlled framework for assessing the capability of numerical methods to reproduce experimentally measured propeller performance. The Duisburg Propeller Test Case (DPTC), associated with the DTC benchmark, has subsequently been used in detailed numerical and experimental investigations.

Wielgosz et al. (2019) conducted a series of quantitative and qualitative experiments on the Duisburg Propeller Test Case and used the resulting measurements to validate CFD predictions of open-water performance and cavitations patterns. Their work also emphasized the importance of verification and validation when numerical predictions are compared with experimental observations.

Similarly, Dogrul et al. (2018) investigated the hydrodynamic performance of the DTC using CFD and applied grid-convergence and uncertainty analysis procedures to the open-water propeller calculations. These studies demonstrate the usefulness of the DTC/DPTC configuration as a benchmark for evaluating numerical approaches in marine hydrodynamics.

The accuracy of RANS-based propeller simulations is influenced by several numerical and physical modelling choices, including mesh resolution, and the treatment of the near-wall flow (Kim et Leong, 2021).

Baltazar et al. (2020) compared RANS predictions using the k−ω SST turbulence model and a transition model with experimental measurements of the boundary-layer flow over a marine propeller. Their results demonstrated the capability of RANS approaches to reproduce important characteristics of the propeller blade flow, while also highlighting the influence of turbulence and transition modeling on local flow predictions.

In addition, Baltazar et al. (2020) investigated propeller performance over a wide range of Reynolds numbers using a RANS solver and examined the effects of turbulence and transition modeling on the predicted open-water characteristics. These findings underline the importance of an appropriate numerical setup and systematic verification when applying RANS methods to marine propeller simulations. Although the DTC/DPTC has been investigated in previous numerical and experimental studies, further numerical assessments remain useful for evaluating the capability of commonly used RANS-based CFD methodologies to reproduce the principal hydrodynamic characteristics of the benchmark propeller. In particular, a systematic analysis combining mesh refinement, thrust and torque prediction, open-water efficiency, blade pressure distribution, and downstream wake characteristics can provide a comprehensive assessment of the numerical methodology (Firouzi et al., 2022). This study focuses on the prediction of the open-water performance coefficients, including thrust coefficient, torque coefficient, and open-water efficiency, together with the analysis of blade pressure distribution, pressure coefficient distribution, and downstream wake characteristics. The numerical results are compared with available experimental data to assess the capability of the adopted CFD methodology.

METHODOLOGY

Propeller Geometry

The investigated propeller is the Duisburg Test Case (DTC) propeller, which is widely used as a benchmark configuration for the numerical and experimental investigation of marine propeller hydrodynamics. The propeller considered in the present study is a five-bladed propeller with a diameter of ($D = 0.25$ m), operating under uniform inflow conditions. The geometry was reconstructed from the available DTC design data, preserving the principal geometric characteristics of the original benchmark propeller. The reconstructed propeller geometry was subsequently imported into the computational domain and used for the numerical simulations. The propeller was considered under open-water conditions, and its hydrodynamic performance was evaluated over a range of advance coefficients. The main performance parameters considered in the present study are the thrust coefficient (K_T), torque coefficient (K_Q), and open-water efficiency (η_0). The DTC propeller geometry and the corresponding experimental data provide a suitable reference for assessing the accuracy of the adopted CFD methodology. The experimental benchmark is therefore used for the validation of the numerical predictions presented in the following sections. 2.2. Computational Domain and Mesh Generation The computational domain was constructed to represent the open-water operation of the DTC propeller under uniform inflow conditions. The domain consists of a cylindrical rotating region surrounding the propeller, allowing the rotational motion of the propeller to be treated separately from the stationary outer flow region. The computational geometry and mesh were generated using ANSYS ICEM CFD. A structured mesh was generated with increased mesh resolution in the vicinity of the propeller blades in order to adequately capture the strong velocity and pressure gradients near the blade surfaces. Particular attention was given to the near-wall region, where boundary-layer refinement was applied. The mesh quality was also monitored to ensure a suitable discretization for the subsequent RANS calculations. Several mesh densities were examined, and the mesh containing approximately 1.5 million cells was selected for the final simulations based on the stability of the predicted hydrodynamic coefficients. The k–ω SST turbulence model was adopted for the final calculations based on its suitability for the prediction of turbulent flow around the propeller blades. The dimensionless wall distance was maintained at ($y+ < 30$) over the blade surfaces. The final computational mesh and the corresponding propeller geometry are presented in Figure 1.

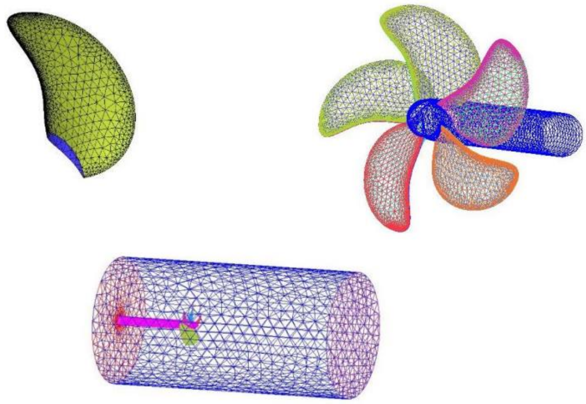

Fig.1. Domain and propeller mesh Generation.

Numerical Setup

The numerical simulations were performed using the ANSYS CFX solver to solve the incompressible Reynolds-Averaged Navier–Stokes (RANS) equations. The k–ω SST turbulence model was employed to model the turbulent flow around the propeller blades. This model was selected to provide an appropriate representation of the near-wall flow and the separated flow regions that may develop around the propeller blades. The computational domain was divided into rotating and stationary regions. The rotational motion of the propeller was represented using the Multiple Reference Frame (MRF) approach, in which the propeller was located within a rotating cylindrical region while the surrounding flow domain remained stationary. The interface between the rotating and stationary regions was treated to transfer the flow variables between the two domains. For the open-water simulations, a uniform velocity inlet was prescribed upstream of the propeller, with the inlet velocity varied according to the investigated advance coefficient. A static pressure condition was imposed at the outlet, while no-slip boundary conditions were applied on the propeller blade and hub surfaces. The remaining external boundaries were treated according to the computational-domain configuration. The simulations were performed under steady-state conditions. Convergence was assessed based on the reduction of the numerical residuals together with the stability of the calculated thrust and torque coefficients. A residual convergence criterion of 10^{-5} was adopted, and the solution was considered converged when the monitored hydrodynamic quantities reached stable values.

Validation Approach

The numerical predictions were validated against available experimental data for the Duisburg Test Case propeller under open-water conditions. The validation was performed by comparing the predicted thrust coefficient K_T, torque coefficient K_Q, and open-water efficiency η0 with the corresponding experimental data over the investigated range of advance coefficients, $0.1 \leq J \leq 1.0$. For each advance coefficient, the relative deviation between the CFD and experimental results was calculated for the three hydrodynamic performance parameters. The results show that the numerical predictions reproduce the overall trends of the experimental propeller characteristics, although noticeable differences are observed at several operating conditions.

Table 1. Numerical and Experimental values of K_T, $10K_Q$, and η_0, together with the corresponding relative deviations.

	CFD			**EXPERIMENT**			**ERROR %**		
J	K_T	$10K_Q$	η_0	K_T	$10K_Q$	η_0	K_T	$10K_Q$	η_0
0.1	0.631	0.923	0.108	0.472	0.667	0.113	33.71	38.38	04.42

0.2	0.409	0.647	0.201	0.427	0.613	0.222	04.42	05.54	09.45
0.3	0.291	0.492	0.283	0.378	0.554	0.326	22.77	11.19	13.19
0.4	0.328	0.548	0.381	0.327	0.423	0.423	0	29.55	09.92
0.5	0.241	0.429	0.447	0.276	0.430	0.511	12.52	0.232	12.52
0.6	0.194	0.364	0.510	0.225	0.366	0.586	13.422	0.546	12.96
0.7	0.150	0.302	0.550	0.172	0.299	0.642	12.55	1.003	14.33
0.8	0.103	0.241	0.544	0.118	0.228	0.656	12.71	5.701	17.07
0.9	0.050	0.170	0.422	0.058	0.151	0.553	13.27	12.58	23.68
1.0	0.012	0.085	0.229	0.009	0.065	0.209	33.33	30.76	9.65

The mean relative deviations over the investigated range are approximately 15.9% for K_T, 13.5% for $10K_Q$, and 12.7% for η_0. The magnitude of the deviation varies with the advance coefficient. For example, a close agreement is obtained for K_T at J = 0.4, while the deviation in $10K_Q$ is relatively large at the same operating condition. Conversely, at J = 0.5, the predicted $10K_Q$ is very close to the experimental value, whereas a larger difference is observed for K_T. The observed discrepancies may be attributed to several factors, including the adopted turbulence model, spatial discretization, numerical treatment of the rotating flow, and differences between the numerical representation and the experimental conditions. Nevertheless, the CFD results capture the principal variation of the propeller performance coefficients with advance coefficient and provide a basis for the subsequent analysis of the propeller flow field.

RESULTS AND DISCUSSION

Thrust and Torque Coefficients

The predicted thrust and torque coefficients of the DTC propeller were evaluated over the advance coefficient range $0.1 \leq J \leq 1.0$ and compared with the available experimental data. Figure 2 presents the variations of K_T and $10K_Q$ as a function of the advance coefficient. The numerical results reproduce the general decreasing trend of both thrust and torque coefficients with increasing advance coefficient. The predicted K_T decreases from 0.631 at J = 0.1 to 0.012 at J =1.0, while $10K_Q$ decreases from 0.923 to 0.085 over the same range. This behavior is consistent with the expected reduction in propeller loading as the advance coefficient increases.

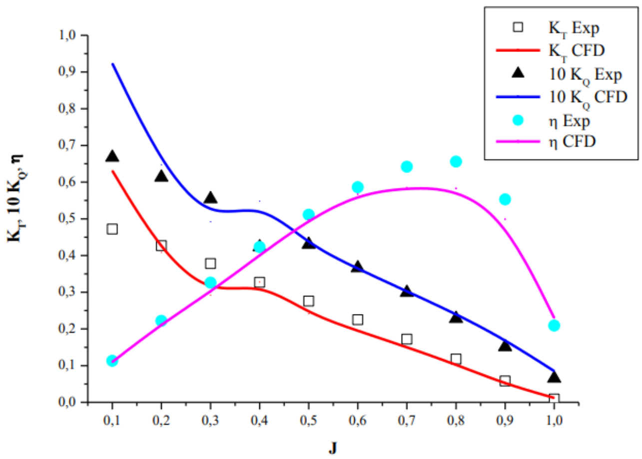

Fig.2. Comparison of the predicted and experimental propeller performance coefficients as a function of advance coefficient.

A comparison with the experimental data shows that the level of agreement varies with the operating condition. For K_T, the numerical and experimental results are very close at $J = 0.4$, where the relative deviation is approximately 0%, whereas larger deviations are observed at J = 0.1, 0.3, and 1.0. For $10K_Q$, particularly good agreement is obtained at $J = 0.5$–0.7, with deviations of approximately 0.23%, 0.55%, and 1.00%, respectively. However, larger discrepancies occur at some other advance coefficients. Over the complete investigated range, the mean absolute deviations are approximately 15.9% for K_T and 13.5% for $10K_Q$. These deviations indicate that, although the numerical model captures the overall trends of the propeller performance characteristics, differences between the CFD predictions and experimental measurements remain at several operating conditions. The observed discrepancies may be related to the mesh resolution, numerical treatment of the rotating flow, and differences between the computational and experimental conditions. Nevertheless, the predicted trends of K_T and $10K_Q$ provide a consistent representation of the variation of propeller loading with advance coefficient.

Open-Water Efficiency

The open-water efficiency η_0 was evaluated from the predicted thrust and torque coefficients and compared with the available experimental data over the investigated range of advance coefficients. The corresponding results are presented in Figure 2. The numerical results show that the open-water efficiency increases with increasing advance coefficient over the lower part of the investigated range, reaches a maximum value of approximately 0.55 at J =0.7, and subsequently decreases as the advance coefficient is further increased. The experimental results exhibit a similar general behavior, with a maximum efficiency of approximately 0.64 at $J = 0.7$. Although the CFD predictions reproduce the general variation of the open-water efficiency with advance coefficient, the numerical values are generally lower than the experimental measurements over most of the investigated range. The difference is particularly noticeable at higher advance coefficients.

The relative deviations in η_0 range from approximately 4.4% to 23.7%, with the largest deviation occurring at $J = 1$. The discrepancy between the numerical and experimental efficiency may be associated with the differences observed in the predicted thrust and torque coefficients, since the open-water efficiency is directly determined from these two quantities according to equation 1 :

$$\eta_0 = \frac{J\, K_T}{2\,\pi\, K_Q} \quad (1)$$

Therefore, the accuracy of the predicted efficiency depends simultaneously on the numerical prediction of thrust and torque. Despite the observed quantitative differences, the CFD results reproduce the main trend of the experimental open-water efficiency curve.

Pressure Distribution and Blade Loading

The pressure distribution over the propeller blade surfaces was investigated for different advance coefficients in order to examine the variation of the blade loading under open-water conditions. Figure 3 presents the pressure contours on the intrados and extrados surfaces for J = 0.1 to 1.0.

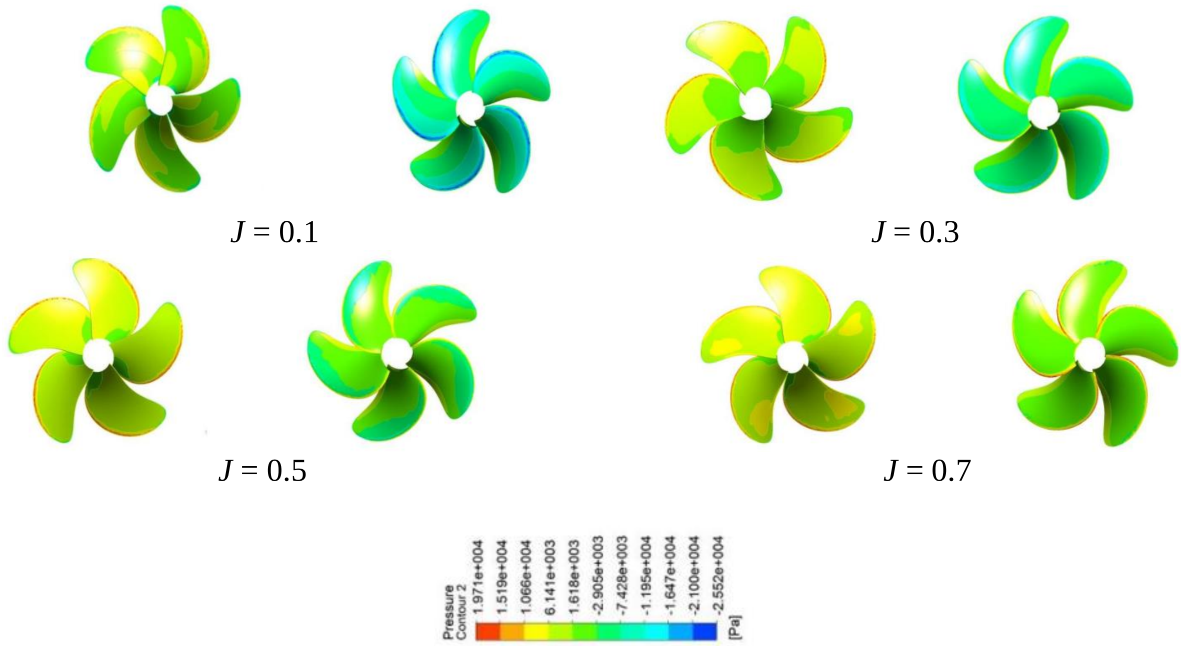

Fig.3. Pressure contours on the intrados and extrados surfaces of the DTC propeller for different advance coefficients.

Note: The extrados is shown on the right, whereas the intrados is shown on the left.

The pressure contours show a clear difference between the pressure levels on the intrados and extrados surfaces. At lower advance coefficients, the pressure difference between the two blade surfaces is more pronounced, indicating higher hydrodynamic loading on the propeller blades. As the advance coefficient increases, this pressure difference becomes less pronounced, indicating a progressive reduction in blade loading, which is consistent with the decrease in the thrust coefficient K_T.

The pressure distribution also varies along the blade radius, with the strongest pressure variations occurring mainly near the leading-edge and loaded regions of the blades. The pressure contours remain relatively similar from blade to blade, reflecting the periodic nature of the flow around the five-bladed propeller. At higher advance coefficients, the pressure difference between the intrados and extrados surfaces become generally weaker, which is consistent with the reduction in K_T and K_Q observed in the open water performance results. These pressure distributions provide further insight into the hydrodynamic loading responsible for the predicted thrust and torque characteristics.

Wake Flow Analysis

The downstream wake field was investigated to characterize the flow structures generated by the rotating propeller. Figure 4 presents the velocity streamlines in the downstream region of the DTC propeller. The wake exhibits a distinct helical structure resulting from the rotational motion of the propeller blades. The streamlines reveal the development of coherent swirling structures downstream of the propeller, particularly in the regions associated with the blade tips and the propeller hub.

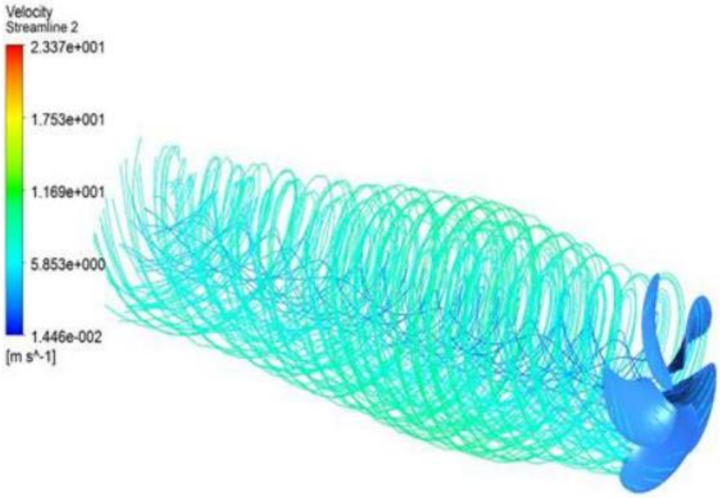

Fig.4. Velocity streamlines illustrating the downstream wake structure of the DTC propeller.

The helical wake structure remains visible downstream of the propeller, while the flow structures gradually evolve as they are convected downstream. These features are characteristic of the rotational flow generated by a marine propeller and provide further insight into the three-dimensional nature of the propeller wake.

Pressure Coefficient Distribution

Figure 5 presents the pressure coefficient Cp distribution along the blade chord at the radial position r = 0.7R for the investigated advance coefficients, $0.1 \leq J \leq 1.0$. The distributions illustrate the variation of the pressure loading between the two sides of the propeller blade under different operating conditions.

At low advance coefficients, corresponding to higher propeller loading, a pronounced difference is observed between the pressure coefficient distributions on the pressure and suction sides, particularly near the leading-edge region. The strong pressure difference between the two blade surfaces contributes to the generation of propeller thrust.

As the advance coefficient increases, the difference between the pressure coefficient distributions on the two blade surfaces generally becomes less pronounced. This behavior indicates a progressive reduction in the hydrodynamic loading of the blade, which is consistent with the decrease in the thrust coefficient KT observed in the open-water performance results.

The largest variations in Cp occur near the leading edge, where the blade experiences a strong interaction with the incoming flow. Moving toward the trailing edge, the pressure coefficient distributions on the two surfaces progressively approach each other, indicating a reduction in the pressure difference along the chord. This behavior becomes more evident at higher advance coefficients.

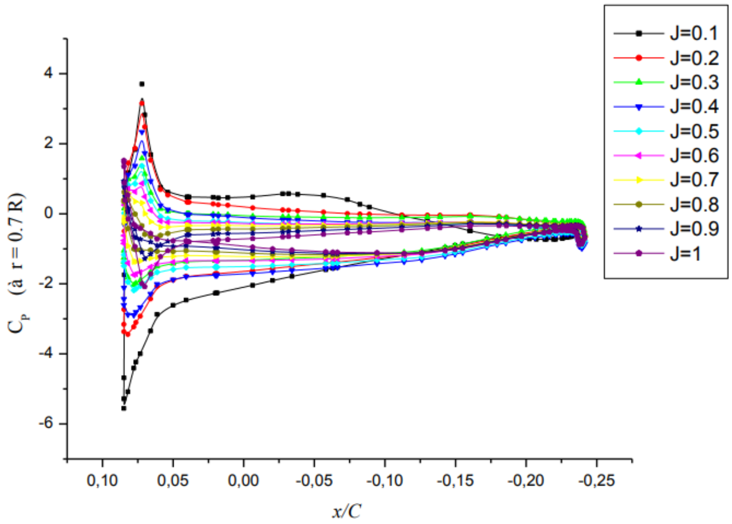

Fig.5. Pressure coefficient distribution along the blade chord at r = 0.7R for different advance coefficients.

Overall, the pressure coefficient distributions demonstrate the dependence of blade pressure loading on the advance coefficient. The reduction in the pressure difference between the suction and pressure sides with increasing *J* is consistent with the observed reduction in propeller thrust and torque.

CONCLUSION

This study presented a numerical investigation of the hydrodynamic performance of the Duisburg Test Case (DTC) propeller using a RANS-based CFD approach. The propeller geometry was reconstructed and simulated using ANSYS CFX with the k−ω SST turbulence model and the Multiple Reference Frame (MRF) approach. The predicted open-water performance was evaluated in terms of the thrust coefficient K_T, torque coefficient $10K_Q$, and open-water efficiency η_0, and was compared with available experimental data over the investigated range of advance coefficients. The numerical results reproduced the overall trends of the experimental performance characteristics, although noticeable deviations were observed at several operating conditions. The mean absolute deviations over the investigated range were approximately 15.9% for K_T, 13.5% for $10K_Q$, and 12.7% for η_0. The pressure-distribution analysis showed that the blade loading decreases progressively with increasing advance coefficient. At lower J, a larger pressure difference between the two blade surfaces was observed, consistent with the higher thrust generated by the propeller. The pressure coefficient distributions at r/R=0.7 further confirmed the reduction in blade loading as the advance coefficient increased. The downstream wake analysis revealed the characteristic helical flow structures generated by the rotating propeller, including coherent structures in the vicinity of the blade-tip and hub regions. These results provide additional insight into the relationship between propeller loading and the resulting wake development. Overall, the present results demonstrate that the adopted RANS-based CFD methodology is capable of reproducing the principal hydrodynamic trends of the DTC propeller and provides useful information on its performance, blade pressure loading, and downstream wake characteristics.

REFERENCES

Baltazar, J., Melo, D. B., Rijpkema, D. (2020). Analysis of the blade boundary-layer flow of a marine propeller using a RANS solver. Ocean Engineering, 211, 107633. https://doi.org/10.1016/j.oceaneng.2020.107633.

Baltazar, J., Rijpkema, D., Falcão de Campos, J. (2021). Prediction of the propeller performance at different Reynolds number regimes with RANS. Journal of Marine Science and Engineering, 9(10), 1115. https://doi.org/10.3390/jmse9101115.

Carlton, J. S. (2018). Marine Propellers and Propulsion. 4th ed. Oxford, UK: Butterworth-Heinemann. https://doi.org/10.1016/C2014-0-01177-X.

Dogrul, A., Ozdemir, Y. H., Sezen, S., Barlas, B. (2018). Uncertainty assessment and self-propulsion estimation of Duisburg Test Case. 3rd International Symposium on Naval Architecture and Maritime, Istanbul, Turkey.

Firouzi, J., Ghassemi, H., Akbari Vakilabadi, K. (2022). Effect of the cross-flow wake on the hydrodynamic performance of the HSP propeller by the CFD solver. Journal of Marine Engineering & Technology, 21(5), 271–280. https://doi.org/10.1080/20464177.2021.1893136.

Kim, H., Leong, Z. Q. (2021). Numerical testing and verification of a marine propeller operating in a uniform flow field. Ships and Offshore Structures, 16(2), 120–126. https://doi.org/10.1080/17445302.2019.1710917.

Kınacı, Ö. K., Kükner, A., Bal, Ş. (2013). On propeller performance of DTC Post-Panamax container ship. International Journal of Ocean System Engineering, 3(2), 77–89. https://doi.org/10.5574/IJOSE.2012.3.2.077.

ITTC. (2021). Recommended Procedures and Guidelines: Open Water Test, 7.5-02-03-02.1, Revision 04. International Towing Tank Conference.

Wielgosz, C., Golf, R., Lidtke, A. K., Vaz, G., el Moctar, O. (2019). Numerical and experimental study on the Duisburg Propeller Test Case. 22nd Numerical Towing Tank Symposium (NuTTS 2019), Tomar, Portugal.